Available online www.jocpr.com

Journal of Chemical and Pharmaceutical Research, 2024, 16(6):1-19

Research Article

ISSN: 0975-7384
CODEN (USA): JCPRC5

Advances and Challenges in Three-Dimensional Bioprinting Strategies

Nanxi Jing*

Department of Medical and Dental Sciences, University of Birmingham, Birmingham, United Kingdom

Received: *31-MAY-2024, Manuscript No. JOCPR-24-137442;* ***Editor assigned:*** *03-Jun-2024, PreQC No. JOCPR-24-137442 (PQ);* ***Reviewed:*** *17-Jun-2024, QC No. JOCPR-24-137442;* ***Revised:*** *24-Jun-2024, Manuscript No. JOCPR-24-137442 (R);* ***Published:*** *01-Jul-2024, DOI:10.37532/0975-7384.2024.16(6).160*

ABSTRACT

Three-dimensional (3D) Bioprinting is a promising technology to revolutionize the biomedicine and pharmaceutical fields by offering a new approach to producing accurate, functional tissue constructs in a manageable manner. This essay is a systematic review of currently developed 3D bioprinting strategies. Initially, the prerequisites for 3D bioprinting will be presented, including biomedical imaging, computer modeling, and bioink formulation. Subsequently, the fundamental configuration and operational process of four 3D bioprinting techniques, extrusion-based bioprinting, inkjet-based bioprinting, laser-assisted bioprinting, and stereolithography will be expounded. Lastly, the obstacles associated with this technology will be emphasized.

Keywords: Three-Dimensional bioprinting; Tissue engineering; ECM-based materials

INTRODUCTION

Over the past decades, the progress of tissue and organ biology studies remains highly impeded. This is because current approaches of *in vitro* tissue modeling, two-dimensional cell cultures and animal models, are limited due to their inability to fully replicate human physiology and tissue complexity [1]. The biomedicine field desperately needs an *in vitro* biological model that structurally and functionally mimics *in vivo* tissues and organs for experimental uses. Various approaches have been taken by bioengineers to make such replicas. The traditional method for culturing *in vitro* 3D tissue is built on the establishment of an Extracellular Matrix (ECM) system, which provides a solid 3D scaffold for cells to adhere [2]. Growth factors are applied to the matrix to assist cell growth and differentiation [3]. Concentration gradients of growth factors can also help the cells to migrate into certain positions within the matrix [4]. The dynamic

interactions between cells, ECM, and growth factor result in cells forming a 3D architecture that spontaneously emulates real organs and tissues. The high inefficiency and irreproducibility nature of the traditional approach forces scientists to explore new methods to create such models. With the capability of producing precise, customized tissue constructs in a manageable manner, the 3D bioprinting technology has drawn numerous attention in recent years, shown in Figure 1.

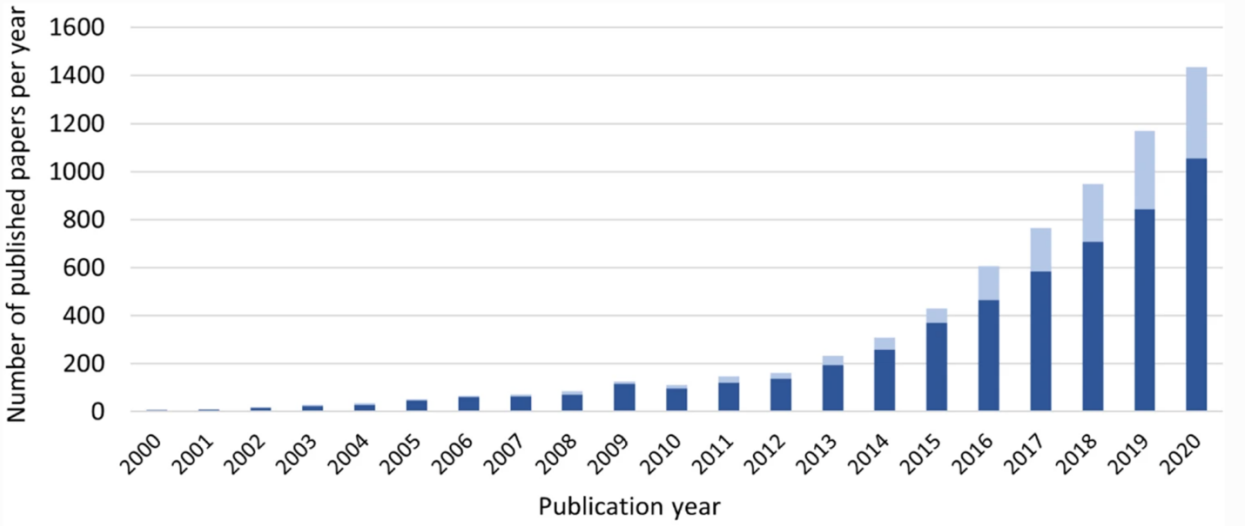

Figure 1: Published reviews and articles that contain the term '3D Bioprinting' from 2000 to 2020. Note: (■): 3D bioprinting-articles; (■): 3D bioprinting-reviews.

As a promising technology that can be used to manufacture artificial models, the field of 3D bioprinting has extended rapidly. 3D Bioprinting allows a layer-by-layer deposition of the bioink, typically a mixture of viable cell types embedded in biomaterials, in a bottom-up fashion [5]. Compared to non-biological 3D printing, 3D bioprinting is more challenging as it involves the printing of cells with materials. This presents some challenges such as the biocompatibility of the chosen material, growth factor delivery, cell viability maintenance, and cell sensitivity to external pressure [6].

The bioprinting process is automated and precisely controlled, cells and growth factors can be selectively seeded onto a meticulously patterned 3D ECM, and thus these cells can then grow into any desired structure that emulates the natural cellular architecture [7]. The accurate geometry and structure of the expected product is created as a 3D computer model before being printed. This precision and manageability give 3D printed organ models a unique advantage in replicating inter and intra-cell-cell communication as well as creating interconnected pores for gas and nutrient perfusion by accurately recapitulating the microniches for each cell type [6]. Applications of 3D bioprinted models can be expanded from *in vitro* models to surgical implants, which will greatly benefit the development of disease modeling, drug screening, and translational tissue engineering.

MATERIALS AND METHODS

Prerequisites for 3D bioprinting

3D bioprinting aims to manufacture a precise structural and functional reproduction of tissues or organs *in vitro* [8]. 3D bioprinting involves three major stages: The preparation stage, the printing stage, and the post-printing stage, shown as in Figure 2. In the preparation stage, a thorough understanding of the microenvironment of the target tissue to be engineered is gained, including the cellular composition including the spatial organization of various cell types, the biophysical characteristics of its extracellular environment, the shape ECM, and the gradient of growth factors. Bioink will be formulated based on this information. As an indispensable tool in 3D printing tissues, biomedical imaging has developed for years as an individual discipline. It provides vital anatomical and physiological information about the target tissue or organ from a cellular level to a whole-organ level [9]. This technology has also been modified and specialized to monitor the interaction between biomaterials and tissues, which further demonstrated its application in the 3D bioprinting [10]. Noninvasive imaging modalities are the most widely used imaging techniques since they do not intervene in the established physiological system. Common examples are Magnetic Resonance Imaging (MRI) and Computed Tomography (CT). Obtained results are analyzed and processed using Computer-Aided Manufacturing (CAD-CAM), which is software that precisely describes the 3D structure of tissues meanwhile predicting the potential mechanical interactions [11]. The digital model will then be linked with the automated 3D bioprinter for manufacturing the desired tissue product. The 3D digital model is then divided into numbers of thin horizontal 2D cross-sectional slices, with each containing complete and unique anatomical information. Using the information from each 2D slice, 3D constructs can be assembled from layers of slices deposited together vertically [12]. Bioinks are formulated after the printing path is determined (Figure 2).

Depending on the cellular and a cellular composition of the target tissue, bioprinters are loaded with appropriate bioink. Bioink consists of biocompatible materials, cells, nutrients, and biochemical molecules [5]. Normally, the materials in bioink are required to have multiple properties to fulfill the need of bioprinting such as optimized rheological, mechanical, and biochemical features [13].

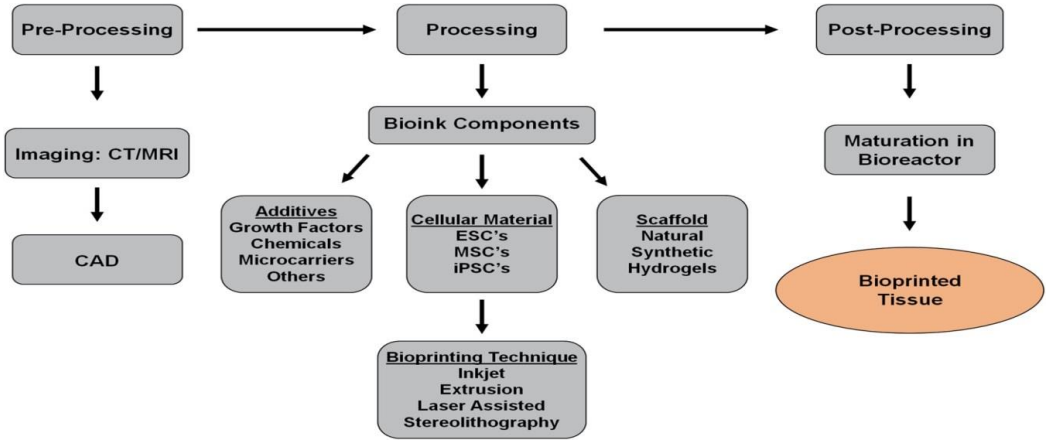

Figure 2: Overview of 3D bioprinting process.

These properties are indispensable in terms of providing essential structural support, creating tissue-specific mechanical robustness, meanwhile maintaining printability and printing fidelity before and after printing. Other than its scaffolding effect, the biomaterials also serve as the 'protection shell' to the laden cells. For example, during the printing stage, mechanical pressure is applied on the bioink and introduces shear stress on cells which can be fatal to cells. The materials can now provide structural support against this stress, preventing cells from harsh environments as well as reducing cell death rate [14]. To date, number of natural polymers has been used in bioinks including collagens, gelatins, alginate, silk and a range of synthetic hydrogels like polyvinyl alcohol, polylactic acid and polyethylene glycol, each exhibiting unique qualities that fit various scenarios [15]. These materials are either photo-crosslinked or thermal-crosslinked to further increase the mechanical stability and resistance of the printed structure [16]. Both of these methods establish chemical bonding of different polymer chains in the material *via* crosslinking agents. In photo-crosslinking, the crosslinking agents are activated by UV light while the activating agents in thermal crosslinking is activated by temperature. Aside from the material part, the cellular compartments have number of origins in preparing bioink. Primary cells can be harvested directly from a patient. Despite the high cost, this type of cell possesses an identical gene expression profile and cellular physiology as patients, which makes it ideal for personalized medicine [17]. Other than primary cell lines, stem cells like embryonic stem cells, Mesenchymal Stem Cells (MSCs), and induced Pluripotent Stem Cells (iPSCs) can also be used for bioink synthesis [14]. Biochemical modifications are encouraged in bioink to provide a microenvironment that promotes cell viability and other cellular behaviors such as proliferation and differentiation [18]. In addition, biochemical molecules like growth factors can also be applied to the material for the spatiotemporal control of tissue growth. The arrangement of specific growth factors is inspired by the development of native tissue. In recent years, improvements in growth factor patterning control have allowed more bioink formulations that better emulate native tissue to be developed. This bioinks contains multiple types of growth factors that are spatiotemporally distributed in the same way as *in vivo* tissue, which encourages the restoration of cell patterning. Coprinting and patterning of different types of bioinks allow engineers to create more complex heterogeneous tissue structures in the lab [5]. The composition and characteristics of bioink are crucial in determining the printing resolution, gelling speed, and mechanical and biological properties of the final product [19]. After proper bioink has been formulated and loaded into the bioprinter, the printing stage can be initiated.

The bioprinter receives the instructing data from computer models and deposits bioink layer-by-layer. The patterning of bioinks is mainly achieved by the moving and alternating of printing nozzles. Currently, there are four major strategies: Extrusion-Based Bioprinting (EBB), Inkjet-Based Bioprinting (IBB), Laser-Assisted Bioprinting (LAB) and stereolithography. Each of them holds different performances in surface resolution, cell density, cell viability, biomaterial viscosity, printing speed, and cost, summarized in (Table 1).

Table 1: A brief summary of the performance of the four bioprinting strategies.

	EBB	**IBB**	**LAB**	**Stereolithography**
Resolution	100 μm	50 μm	10 μm	100 μm
Cell Density	High	Low	Medium	Medium
Cell Viability	89.46% ± 2.51%	80%-95%	<85%	>90%
Biomaterials Viscosity	30-6 × 107 mPa s	<10 mPa s	1-300 mPa s	No limitation
Printing Speed	Slow	Fast	Medium	Fast
Cost	Low	Low	Medium	High

Bioprinting strategies

Extrusion-Based Bioprinting (EBB): EBB is the most popular bioprinting strategy. A typical structure usually contains a bioink handling system controlled by a numerical control system and a planar where the printing material will be deposited [20]. The numerical control system utilizes the input data from prior computer models and controls the motions of the dispensing nozzles along the x, y and z axis. It also gives commands to powering system within the bioink handling nozzles, which will be either pneumatic or mechanical. By digitally maneuvering the driving force, a continuous uninterrupted bioink stream can be pushed out onto the planar. Nozzles are mobile along the z axis while ejecting the bioinks stream to give the 2D structure of the desired layer. Then, the deposited layer will act as the new planar where the new layer will be printed onto, allowing 3D geometry formations. The manner in which different layers' stack is crucial in maintaining the structural steadiness. A vital parameter is the overlapping ratio, which describes the contact area between layers. Typically, the overlapping ratio is between 75% to 100% to prevent delamination [16]. In addition, the planar may rotate for a small angle by each layer to alternate the contact angles and well as creating pores, thus increasing the dragging force between layers to avoid collapse. Varying the spacing between each deposited bioink strand by changing the diameter, moving speed, printing rate, and temperature of the nozzles can also change the mechanical features of the product.

Several nozzle variations of EBB have been developed, each with its own advantages and limitations represented in Figure 3. For example, the pneumatic dispensing nozzle is easy-manipulative and can lower the cost of the whole system, as it contains less and simple compartments while generating a strong driving force, depending on its pressure capacity [21]. However, explicit control of the force cannot be achieved in pneumatic nozzles because the pressing air in the chamber may be delayed. On contrary, the complex structure of a mechanical nozzle offers a descent driving force manageability as there is a collaboration of numbers of complex structures and components [16]. Mechanical nozzles can be further divided into piston-driven nozzles and screw-driven nozzles. The prior one uses a piston to push bioinks out of the syringe. This gives more precise control over the extrusion force and speed, which can result in higher-quality prints. Then latter one utilizes a screw to move the bioinks through the nozzle and

which is particularly useful for extruding viscous bioinks and producing high-resolution products [22]. In addition, these different designs of nozzles can be integrated inside one single bioprinter to achieve coaxial extrusion and multi-material extrusion. Coaxial extrusion involves using two nozzles: an inner nozzle to extrude cell-embedded bioinks and an outer nozzle to extrude supporting biomaterials which will be removed later [23]. Multi-material extrusion allows multiple bioinks or biomaterials with different properties to be printed simultaneously [24]. Both of them are useful for creating complex yet more physiologically relevant structures that include multiple cell types in a single print (Figure 3).

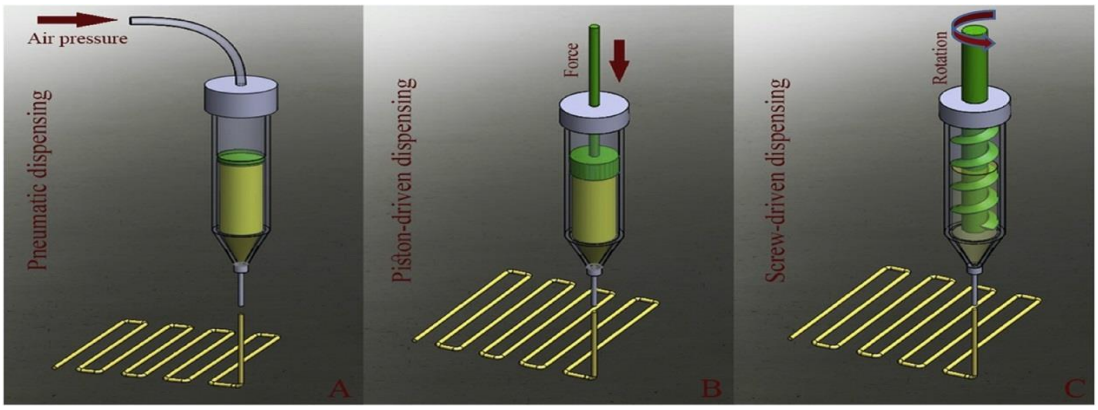

Figure 3: Schematic representation of designs of ebb nozzles. (A) Pneumatic, (B) Piston-driven and (C) screw-driven dispensing method. Pneumatic nozzle deploys compressed air to generate the driving force, while the other two uses mechanical pressure [24].

The most prominent advantage of EBB is its versatility. This bioprinting method is comparably easier to adopt to print a wide variety of biomaterials including hydrogels, copolymers, and cell spheroids [25]. Materials with high viscosity can also be printed to create tough and rigid products. Meanwhile, the printing parameters can be easily customized to fit specific requirements. For example, if the desired product needs high structural integrity, the diameter of the printing head can be increased, the automated control system can reduce the nozzle movements to increase the overlapping of each layer, and a biomaterial with higher viscosity can be used to achieve this goal collaboratively. Aside from this, EBB is the most inexpensive one among all bioprinting methods. This cost-effectiveness, combined with its easy-adapting nature, allows EBB great scalability to produce tissues and organs in large quantities. Despite these advantages, there are also several caveats of this printing method. Firstly, the mechanism that ejecting bioinks can bring negative impacts on cell viability [26]. In order to extrude bioink in a continuous manner, uninterrupted pressure is generated in the syringe and is applied directly to the bioink. This can bring shear force to cells and eventually cause cell death [14]. Luckily, this decrease in cell number can be compensated by its ability to bear bioinks that contain extreme high cell densities. However, there are not any plausible solutions to limitations on the printing resolution of EBBs [27]. A relatively low printing resolution suggests its disability to create descent details of structures, which limits its application to print delicate structures.

Inkjet-based bioprinting: Induced developed in 2003, IBB was derived from conventional inkjet 2D printing [28,29]. Instead of ejecting one continuous stream of bioink like EBB, IBB breaks the bioink into droplets and deposits these drops individually. There are two main categories of IBB-Continuous inkjet bioprinting and Drop-On-Demand (DOD) inkjet bioprinting, graphical representation is shown in Figure 4. In continuous inkjet bioprinting, a flow of bioink is pushed out of the nozzles by controlled pressure which will spontaneously split into individual droplets due to Rayleigh-Plateau instability of fluid [30]. Then, these droplets of bioink will be charged by a charging plate. After this, an electric field is applied to deflect each charged droplet toward its pre-designed position on the substrate. Those excess ones which fail to be charged will be deflected into a recycling system at which they will be collected and reused. Though the recycling process efficiently avoids waste for the whole system, there are chances that the collected bioink is contaminated, which bring negative impacts on the functionality and integrity of the final product. Moreover, the spontaneous nature of the droplet-forming process implies a low manual jurisdiction of the continuous inkjet bioprinting system, which makes it unsuitable for laboratory uses (Figure 4).

On the other hand, DOD inkjet bioprinting allows more precise control over the printing process. The droplet formation in this method is not naturally occurring, but rather follows instructing signals. This controllability has rendered the DOD better accuracy and efficiency, allowing it to adapt a wider application. The charging plate, deflecting electric field, and recycling system are discarded in DOD; instead, its basic structure and workflow are similar to that of EBB. First, the printer receives digital signals from a computer program, where the exact positions within the three-dimensional space of the printing nozzles and the printing modes will be provided for the later printing stage. Then, the bioink contained will be deposited over a piece of 'bio-paper', which is usually made of supporting materials such as hydrogel matrix, culture dish, or any other biocompatible polymer substrates.

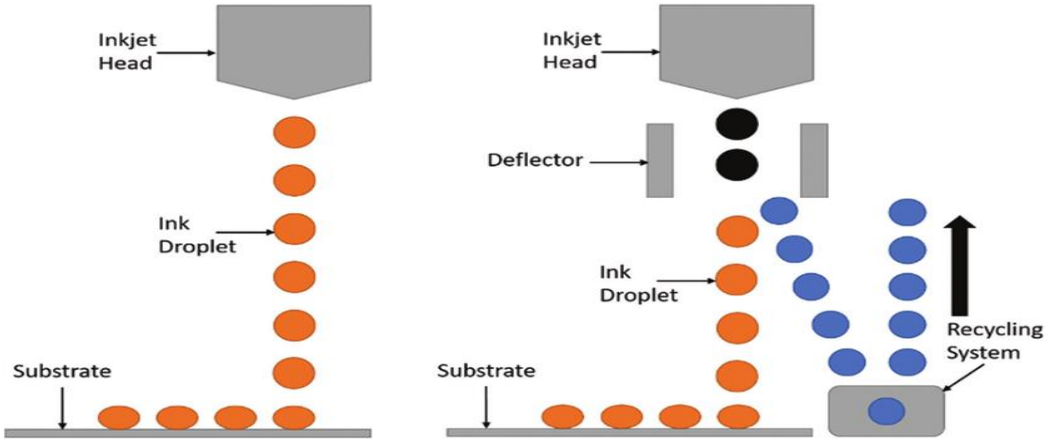

Figure 4: Schematic representation of DOD (left) and continuous inkjet bioprinting (right).

Due to the droplet nature of IBB, pre-programmed pressure pulses are applied instead of a constant continuous pressure to ensure optimized droplet formation [31]. Without pressure, the leaking of bioink can be prevented by surface tension [32].

There are some derivatives of DOD, each holds a unique mechanism to generate droplets, shown in Figure 5. In thermal inkjet bioprinting, a heat actuator is included in the bioink chamber. When the printing signals are received, this structure heats the local bioink for several microseconds, usually with a temperature up to 250°C-350°C. This instantaneous heating process takes place locally, and the overall temperature of the entire bioink will only rise 4°C-10°C [33]. Because of this, the heated local bioink will rapidly vaporize and expand in size to produce heat bubbles, which generate a force to break and eject bioink at the same time. Droplet size created using this method is about 30 μm-80 μm, which is relatively small [34]. Moreover, cell viability is also maintained by this local heating mechanism, the majority of the ejected cell population remains active after printing in compensation of a small amount of cell death caused by the heat [35]. Thermal Inkjet bioprinting is popular for its printing speed and low cost. However, the state of ejected bioink can sometimes be out of control because of the explosion of heat bubbles. Furthermore, because of the small droplet size and nozzle diameter, bioinks with high viscosity do not compile with this method as they may easily cause clogging. Opposingly, piezoelectric inkjet bioprinting allows the production of droplets with larger diameters of 50 μm-100 μm. This method relies on a contracting piezoelectric element to extrude bioink. Typically, the piezoelectric element is bonded to a vibration plate and connected within a circus, located at the end of each printing syringe. When receiving voltage pulses, the bending of the piezoelectric element deforms the vibration plate, hence the volume within the printing syringe suddenly decreases to generate the force that squeezes the bioink out. When the circus is disconnected, the piezoelectric element and the vibration plate return to their original position immediately [36]. Since it is electric driven, the pulsing frequency and magnitude can be easily adjusted to control the droplet formation and improve the printing outcome. The large range of droplet diameter is achieved by a wider print head diameter choice from 18 μm-120 μm [37]. Even though the fatal heat is not involved, there is no significant improvement in cell viability with this method. This could be explained by the negative effect induced by ultrasonic sonication. Sonication with a frequency between 15 kHz-25 kHz is proven to cause cell lysis. Moreover, direct contact between bioink and the vibration plate can also induce shear force and harm cells [6] (Figure 5).

One main advantage of IBB is its precision [38]. The resolution of IBB can reach 2880 dpi × 1440 dpi, depending on the droplet sizes and the distance between two droplets. A precise delivery of desired cell types or proteins to certain locations on the substrate can be achieved using this printing method [39,40]. Using this method, certain cell arrays can be gathered into a specific position to form a mini-functional unit, with many of these functional units ejected by multiple printing nozzles, the functionality of the final product can be greatly improved. This can be particularly useful when creating fine structures at smaller scales, such as fibers and microtubes [41]. Another advantage is its high throughput. This comes from its high ejection frequency and parallel printing manner. Hundreds of nozzles can

eject bioink of different types at high frequency at the same time, allowing a maximized efficiency and printing speed [36]. Nevertheless, this high extruding frequency may lead to droplet splashing and thus affect the printing precision. The droplets ejected from the printing head and hit the substrate with high speed like satellites, this violent clash may break the original shape of the droplet, causing it to expand and lead to a lowered resolution [42]. When it comes to co-bioprinting of different materials and the Marangoni effect may occur to further decrease the resolution.

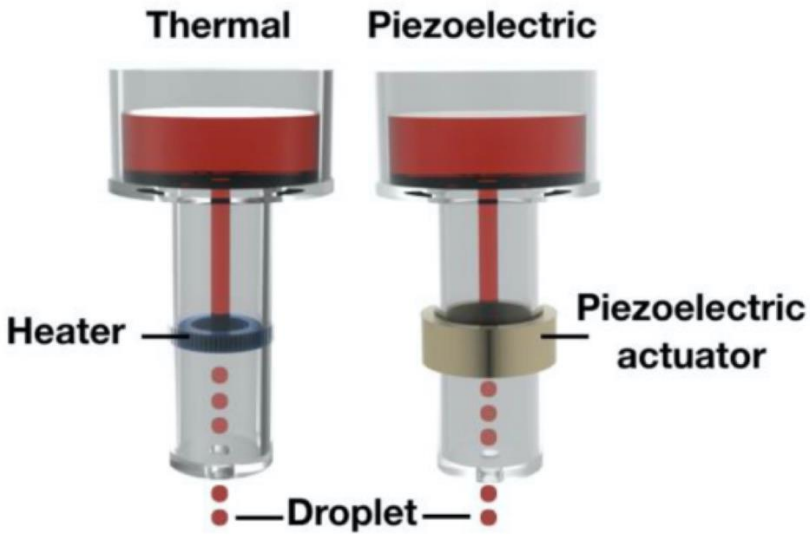

Figure 5: Schematic representations of designs of IBB nozzles. The left one is thermal inkjet bioprinting, the right one is piezoelectric inkjet bioprinting.

Marangoni effect describes the tendency for a liquid drop to spread over another liquid drop which has a higher surface tension [43]. For example, when a high-viscosity bioink droplet is dropped onto a low-viscosity thin film, a crown shape arises vertically and then breaks to form numerous holes which give rise to splashing [44]. Luckily, such effect can be neglectable when printing large tissue/organ level products, however, meticulous control is still required when creating smaller structures. By adjusting the voltage and printing frequency, stable droplets can be created, and the level of splashing can be minimized [45].

Laser-assisted bioprinting: The basis of LAB was first described as Laser-Induced Forward Transfer (LIFT) technology, a method to deposit metal accurately for computer chip fabrications [46]. The common design for LAB involves four main parts: A pulsed laser generator, a module to adjust the laser beam, and a ribbon to contain cell-laden bioink, and a receiving substrate. During the LAB process, the laser beam originating from the automated laser generator is adjusted using mirrors and lenses to focus on a specific position of the bioink layer. A bubble is then generated at the irradiation spot, causing the bioink to stream toward it. The bubble then collapses, creating a high-pressure jet or droplet of bioink that is deposited onto the receiving substrate, allowing the creation of tissue structures [47]. The setup is shown in Figure 6.

A variety of pulsed laser generators has been selected on LAB printers, each emitting laser beam with different wavelengths and pulse durations. A wide range of wavelengths have been tested from 94 nm, 266 nm, 284 nm, 355 nm to 1064 nm, and a preference for the laser with longer wavelengths has been made [48-52].

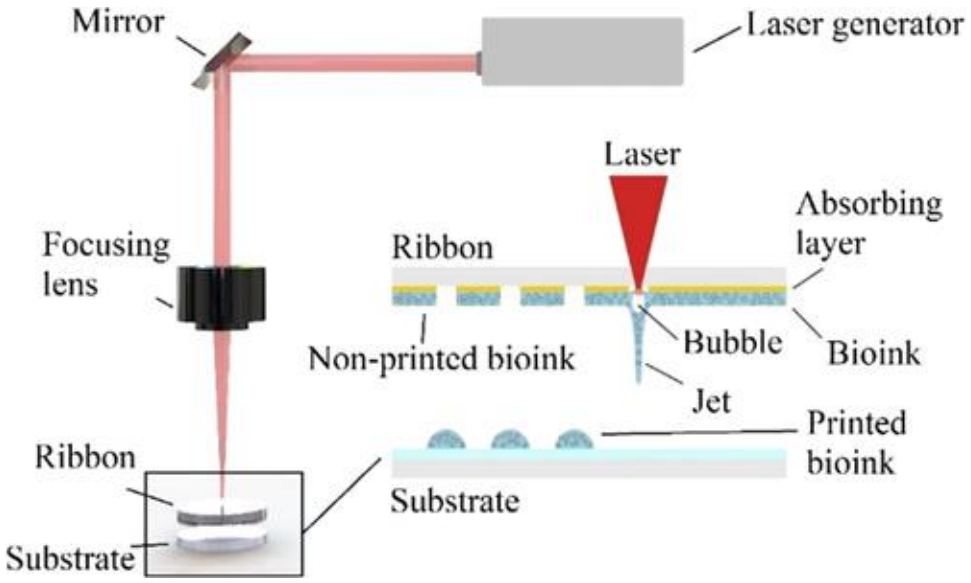

Figure 6: Schematic representation of the basic setup of a LAB biopinter [47].

Selected laser wavelengths such as infrared contain lower energy can therefore cause less effect on the chemical and physical properties of bioink, for example, the crosslinking of materials and the DNA structure within cells. However, infrared laser can have a strong thermal effect which may also impact the cells compared to shorter wavelengths such as Ultraviolet laser. It is believed that shorter pulse duration can reduce this effect. Instead of the most commonly used nanosecond pulse, a femtosecond or a picosecond laser can address the thermal damage problem by shortening the bioink's exposure time to the laser [47].

The ribbon is made up of tightly stacked transparent glass, a thin layer of laser-absorbing material, and a suspended layer of bioink [53]. Among all the components the laser-absorbing layer is the most essential part and intensely researched. This layer aims to benefit the whole system in two ways: (1) It improves the efficiency of laser absorbing [54]. The composing of bioink does not usually consider its ability to absorb radiation energy, without an adequate amount of energy, the jet formation would be significantly rougher and less stable [55]. The laser-absorbing layer can improve the quality of droplets by increasing the rate of absorbing laser energy, (2) This layer also has a protective role for the cells in bioink [56]. Without this layer, cells will be directly exposed to fatal high-energy radiation which leads to a deterioration of cell viability [57]. Typically, the laser-absorbing layer is composed of metal materials with a thickness ranging from 10 nm-100 nm. To date, gold, silver, titanium, and its oxides, have

been reported as the material for this layer [49,58-60]. However, the laser would break this metal layer into fragment and contaminate the bioink. The nanosized metal debris may accumulate within the bioink and eventually bring irreversible toxication to cells [61]. Various attempts have been made to solve this problem, and currently, the most promising one is to replace the metal with a layer of biodegradable material. The broken debris can therefore blend into the other biocompatible materials in the bioink, reducing its impact on cells. In compensation for jetting speed, an absorbing layer made of gelatin was proved to increase cell viability by 10% while reducing 50% of DNA damage [62]. Another approach proposed by Lin and Huang required an additional sacrifice layer. A metallic foil is glued under this sacrifice layer to prevent its broken pieces to enter the bioink. This new method also showed an increase in cell viability and printing resolution [61]. Their design is shown as Figure 7.

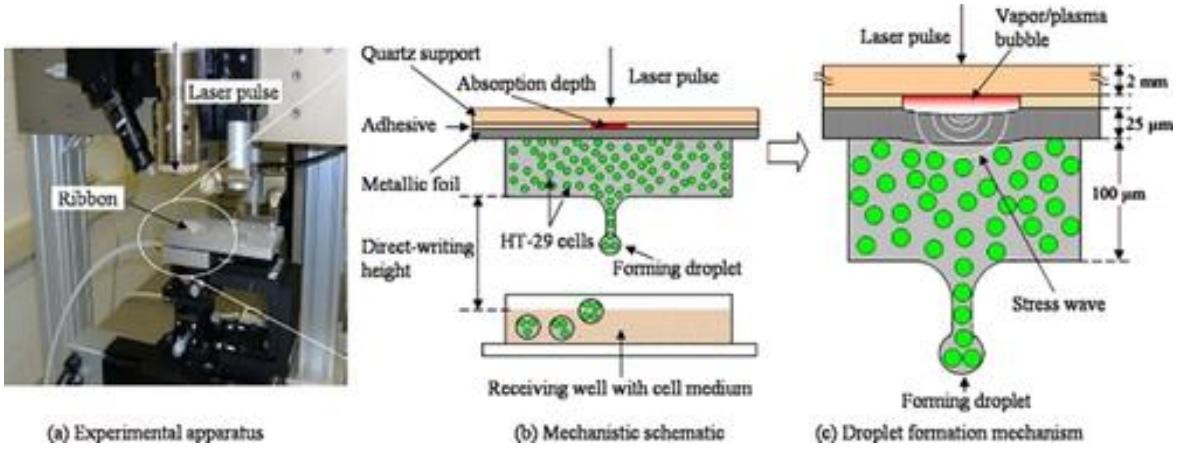

Figure 7: Addition of a sacrifice layer and a metallic foil to increase cell viability in LAB [61].

The LAB is known for its high resolution, which variance depends on factors such as the thickness of the bioink layer coated onto the ribbon, viscosity, and surface tension of the bioink, wettability of the substrate, laser, an air gap between ribbon and substrate, and structural organization [63]. In addition, the method also allows the extrusion of bioink with high viscosity meanwhile guaranteeing maximum cell viability (>95%) since there is no direct physical pressure applied to the bioink [64]. On the other hand, its caveat is also obvious. Setting up LAB system can be very costly. Nevertheless, the expenses associated with 3D printing technologies are decreasing at a rapid rate due to increased demand and supply. This is because there is a growing need for the production of intricate bioengineered tissue constructs in today's world.

Stereolithography: Stereolithography, shown in Figure 8, is another bioprinting approach that utilizes light-based technologies. The system of stereolithography is established based on the idea of selectively transforming the physical state materials from liquid to solid *via* photo-crosslinking in a layer-by-layer manner [65]. Instead of having mobile printing heads like other bioprinting methods, stereolithography printers have computer-controlled receiving stages that move along the z axis, which locates beneath a bioink reservoir. The bioink employed in stereolithography must contain photo-crosslinking agents to initiate the solidification process, such as polyethylene

and its acrylate derivatives [66]. A beam projector cast light beams with set patterns on the bioink reservoirs to these partially polymerize it to produce the desired 2D shape, which will be stacked together to generate the final 3D structure (Figure 8). The illumination of the beam projector is the key in defining the performance of a stereo lithography printer. It determines the resolution of the printing as well as the mechanical properties of the biomaterials [67].

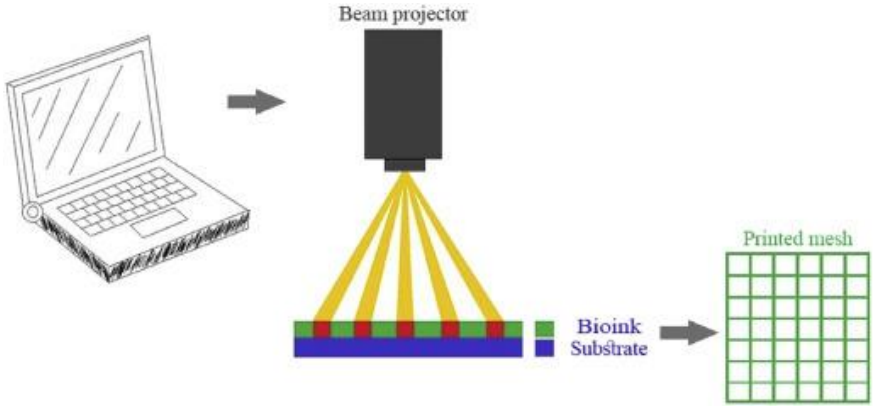

Figure 8: Schematic diagram of stereolithography using beam projector. The pattern of printed mesh depends on the pattern of automated projected beam.

Depending on the number of photons emitted, stereolithography can be classified as single-photon and multiphoton photons. In the single-photon method, one high-energy photon is launched and absorbed by the photo-crosslinking initiators within the bioink to generate free radicals. Its wavelength falls within ultraviolet light and visible light for high energy. However, this high energy may damage the DNAs within the cellular components. To avoid unnecessary cell loss, the multiphoton method emerges. Photons in this method are low-energy and have longer wavelengths such as infrared they hit the initiators one by one to generate enough energy to initiate the polymerization reaction [68,69]. The emission of these photons is patterned to give complexity to the products, known as maskless projection. A structure containing digitally controlled mirror arrays in thickness of 5 μm-10 μm, known as a dynamic mask, rotates collaboratively to manipulate the reflection light beam [70]. The orientation of each mirror within the dynamic mask is controlled by signals from previous scanning and modeling results. Focus lenses can also be added to further enhance the resolution of pattern projection.

Because there is an absence of complicated printing head movements, stereolithography has the fastest bioprinting speed among all four bioprinting methods discussed. This mechanism also allowed the printing of extremely complex patterns. Meanwhile, stereolithography is also a non-contact method that avoids shear force generation, which results in a comparably high cell viability. (>85%) A significant drawback of this system is that the liquid used must be transparent and have limited scattering. If the liquid doesn't meet this requirement, the light won't pass through the material uniformly, which will result in uneven crosslinking. Consequently, the density of cells within the bioink is restricted to about 108 cells per milliliter [64]. Despite this limitation, stereolithography has attracted to

the attention of many research areas because it can bioprint structures quickly without subjecting the cells to shear forces and with a high resolution of approximately 1 μm [71].

RESULTS AND DISCUSSION

From decades of development of 3D bioprinting, this diverse technology has been expanding to become a large market from $2.2 billion in 2012 to $10.8 billion in 2021 [72]. A wide range of tissues from bone to kidneys has been created *via* 3D bioprinting, according to Figure 9. Despite this, there are still several challenges to be solved within this field of study (Figure 9).

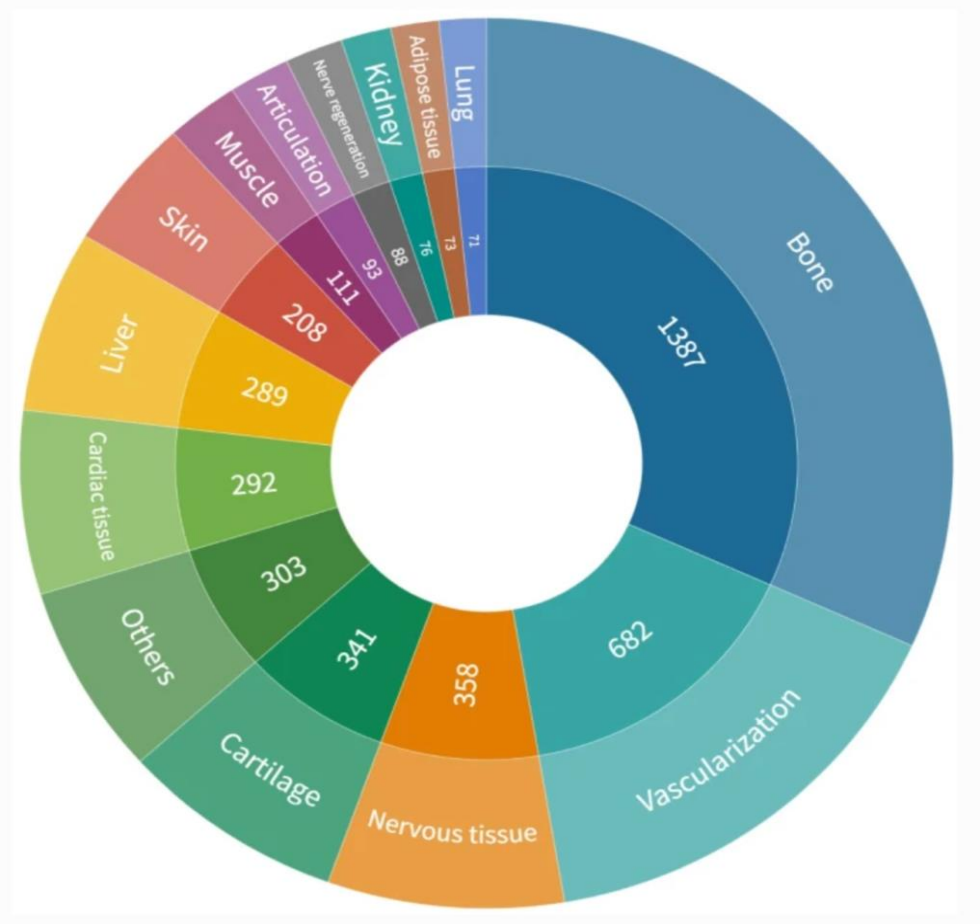

Figure 9: A record of all published works that contains certain keyword in titles related to various *in vitro* tissues and organs in the field of 3D bioprinting. Note: The total number of publications is not equivalent to the sum of tissues/organs listed, as some papers may cover multiple tissues.

For starters, the size of the printed product is limited at this stage because there is no plausible way for nutrient transport and gas exchange for inner cells. To date, the major way to power printed tissue is *via* the diffusion of nutrients through pores, which is highly inefficient. This limitations has been restricting the size and complexities of the printed tissue structures. It is necessary to create a fully functional vasculature system on any printed product to ensure adequate nutrient exchange and waste removal [73]. There have been attempts to add a vascular network to a printed tissue. The first approach is to add an additional layer containing only blood vessel alike channels between two deposited layers, noted as Figure 10. This method involves forming a groove or channel in a single layer, followed by the alignment and deposition of a second layer, resulting in the creation of laminated channels or grooves in a step-by-step process [74]. A disadvantage of this solution is that it takes a significant amount of time for the channel layer to start working, making it difficult to sustain cell viability until it is fully operational. An alternative strategy is to use sacrificial materials instead. The sacrificial materials are utilized during the printing process to create vascularization-like channels and offer structural support for each layer. Later, these materials are eliminated from the final product during a post-processing stage. However, this method will increase the standard of synthesizing bioink, since additional materials for channel formation such as carbohydrate glass (Figure 11) and gelatin need to be added [74] (Figures 10 and 11).

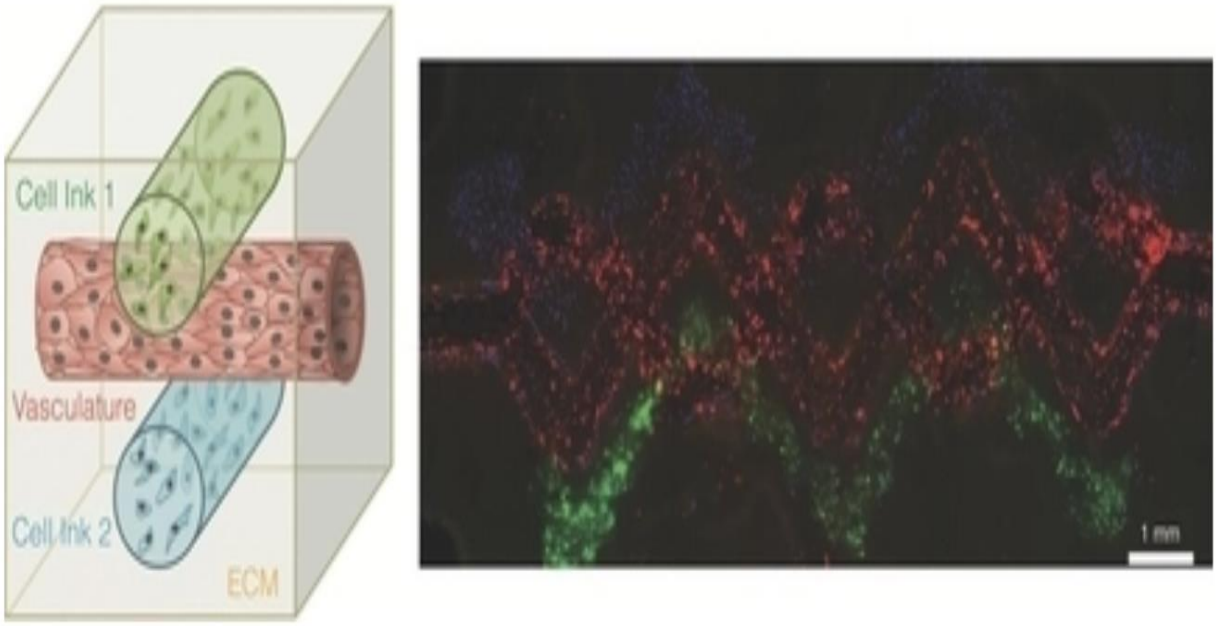

Figure 10: Bioprinting additional vasculature layer. On left is the schematic representation of vasculature's location in between two printed layers. On right is the observed printed construct with vascular system using three fluorescent channels: 10T1/2 fibroblasts (blue), human neonatal dermal fibroblasts (green), human umbilical vein endothelial cells (red) [74].

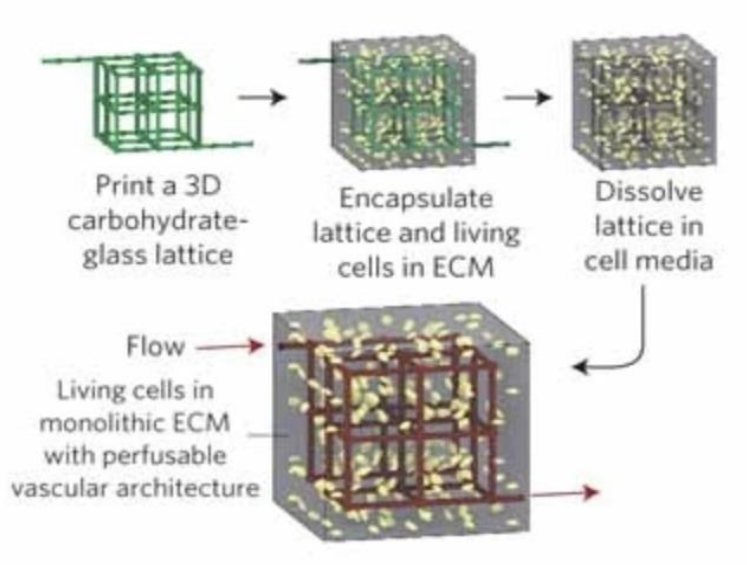

Figure 11: A schematic overview of carbohydrate glass latte as the sacrifice material. This structure is encapsulated with living cells and ECM, and it dissolves quickly in cell media without harming neighboring cells. As a result, a solid tissue construct with a vascular structure that corresponds to the initial carbohydrate-glass lattice is generated [74].

Not to mention the bioink formulation it is already being a concern. Numerous bioinks have been extensively studied for their potential in creating biomimetic tissues. However, despite progress made in inducing organ-like behavior of cells, these synthetic environments often fall short of mimicking the complete composition of the natural organ-specific ECM. In order to address this issue, decellularized ECM (dECM) offers a promising solution, as it can be directly obtained from the desired tissue, including all of the characteristic molecules and growth factors. However, dECM in bioprinting applications is often based on donor organs from animals, which may not fully replicate the natural ECM found in human tissues. Additionally, the process of retrieving, purifying, and modifying the matrix can be time-consuming, and the amount of bioink that can be obtained is limited [75]. Nevertheless, dECM remains one of the most promising sources for achieving bioinks that are capable of fully mimicking the complex environment and composition of realistic tissues, and further research could lead to wider application of dECM in bioprinting.

Another challenge for bioprinting is that it gets clumsy in mimicking the complexity and functionality of natural organs due to low resolution compared to natural tissues and limitations in encapsulating cells. Current bioprinting systems are mostly limited to 3-4 types of cells, whereas natural tissues have more cell types and possess constant cell-cell crosstalk. Coculturing multiple cells in a single bioprinted tissue requires optimizing culture conditions for individual cells, which is exceptionally challenging due to the tissue-specific microenvironment requirements of all cells. Fundamental research is needed to improve culture conditions for the proper maturation of multicellular 3D bioprinted tissues.

CONCLUSION

3D bioprinting is a technology that uses 3D printing to create living tissues, organs, and structures. It has numerous applications in different fields such as tissue engineering, drug testing, personalized medicine, and prosthetics. In this review, four major strategies including EBB, IBB, LAB, and stereolithography are introduced. Their characteristics are also presented along with pros and cons. Meanwhile, the limitations on the size and complexity of the final product urgently need to be solved. As technology advances, the synergy between 3D bioprinting and other technologies can bring new promises in this field of study. More promising applications are expected to emerge using 3D bioprinting methods. In general, despite 3D bioprinting is an advanced method of creating three-dimensional structures using cells that hold great promise, this technology still faces various difficulties and obstacles that need to be overcome.

REFERENCES

[1] Ma C, Peng Y, Li H, et al. *Trends Pharmacol Sci*. 2021;42(2):119-133.

[2] Ehrmann RL, Gey GO. *J Natl Cancer Inst*. 1956;16(6):1375-1403.

[3] Rossi G, Manfrin A, Lutolf MP. *Nat Rev Genet*. 2018;19(11):671-687.

[4] Yu F, Hunziker W, Choudhury D. *Micromachines (Basel)*. 2019;10(3):165.

[5] Abbasov, I.B. *Crit Rev Biomed Eng*. 2022;50(3):19-34.

[6] Murphy SV, Atala A. *Nat Biotechnol*. 2014;32(8):773-785.

[7] Xiong Z, Yan Y, Zhang R, et al. *Scr Mater*. 2001;45(7):773-779.

[8] Ingber de, Mow VC, Butler D, et al. *Tissue Eng*. 2006;12(12):3265-3283.

[9] Codari M, de Cecco CN, et al. Br J Radiol. 2020;93(1113):20190770.

[10] Zhang YS, Yao J. Trend Biotechnol. 2018;36(4):403-414.

[11] Horn TJ, Harrysson OL. *Sci Prog*. 2012;95(3):255-282.

[12] Virzì A, Muller CO, Marret JB, et al. *J Digit Imaging*. 2020;33(1):99-110.

[13] Lee HJ, Kim YB, Ahn SH, et al. *Adv Healthc Mater*. 2015;4(9):1359-1368.

[14] Blaeser A, Duarte Campos DF, Puster U, et al. *Adv Healthc Mater*. 2016;5(3):326-333.

[15] Bartolo P, Malshe A, Ferraris E, et al. *CIRP Annals*. 2022;71(2):577-597. [Crossref] [Google Scholar]

[16] Placone JK, Engler AJ. *Adv Healthc Mater*. 2018;7(8):1701161. [Crossref] [Google Scholar] [PubMed]

[17] Moghaddam AS, Khonakdar HA, Arjmand M, et al. *ACS Appl Bio Mater*. 2021;4(5):4049-4070.

[18] Freeman S, Calabro S, Williams R, et al. *Front Bioeng Biotechnol*. 2022;10:913579.

[19] Jain S, Fuoco T, Yassin MA, et al. *Biomacromolecules*. 2019;21(2):388-396.

[20] Naghieh S, Chen X. *J Pharm Anal*. 2021;11(5):564-579.

[21] Chang CC, Boland ED, Williams SK, et al. *J Biomed Mater Res B Appl Biomater*. 2011;98(1):160-170.

[22] Bhattacharyya A, Janarthanan G, Tran HN, et al. *J Chem Eng*. 2021;415:128971.

[23] Lian L, Zhou C, Tang G, et al. *Adv Healthc Mater*. 2022;11(9):2102411.

[24] Ravanbakhsh H, Karamzadeh V, Bao G, et al. *Adv Mater*. 2021;33(49):2104730.

[25] Jones N. *Nature*. 2012;487(7405):22-23.

[26] Chen DX. *Springer Sci Rev*. 2019. 2018:117-145.

[27] Heinrich MA, Liu W, Jimenez A, et al. *Small*. 2019;15(23):1805510.

[28] Tuan RS, Boland G, Tuli R. *Arthritis Res Ther*. 2002;5:1-4.

[29] Singh M, Haverinen HM, Dhagat P, et al. *Adv mater*. 2010;22(6):673-685.

[30] Rayleigh L. *P Lond Math Soc*. 1878;1(1):4-13.

[31] Agarwal S, Saha S, Balla VK, et al. *Front Mech Eng*. 2020;6:589171.

[32] Derby B. *Annu Rev Mater Res*. 2010;40:395-414.

[33] Cui X, Boland T, DD'Lima D, et al. *Recent Pat Drug Deliv Formul*. 2012;6(2):149-155.

[34] Cui X, Dean D, Ruggeri ZM, et al. *Biotechnol Bioeng*. 2010;106(6):963-969.

[35] Xu T, Jin J, Gregory C, et al. *Biomaterials*. 2005;26(1):93-99.

[36] Wijshoff H. *Phys Rep*. 2010;491(4-5):77-177.

[37] Christensen K, Xu C, Chai W, et al. *Biotechnol Bioeng*. 2015;112(5):1047-1055.

[38] Cui X, Gao G, Qiu Y. *Biotechnol Lett*. 2013;35:315-321.

[39] Ker ED, Chu B, Phillippi JA, et al. *Biomaterials*. 2011;32(13):3413-3422.

[40] Ilkhanizadeh S, Teixeira AI, Hermanson O. *Biomaterials*. 2007;28(27):3936-3943.

[41] Nakamura M, Iwanaga S, Henmi C, et al. *Biofabrication*. 2010;2(1):014110.

[42] Xu Q, Basaran OA. *Phys Fluids*. 2007;19(10).

[43] Thoroddsen ST, Etoh TG, Takehara K. *J Fluid Mech*. 2006;557:63-72.

[44] Aljedaani AB, Wang C, Jetly A, et al. *J Fluid Mech*. 2018;844:162-186.

[45] Yasui T, Inoue Y, Naito T, et al. *Anal Chem*. 2012;84(21):9282-9286.

[46] Bohandy J, Kim BF, Adrian FJ. *J Appl Phys*. 1986;60(4):1538-1539.

[47] Dou C, Perez V, Qu J, et al. *Chem Bio Eng Rev*. 2021;8(5):517-534.

[48] Nguyen AK, Narayan RJ. *Ann Biomed Eng.* 2017;45(1):84-99.

[49] Othon CM, Wu X, Anders JJ, et al. *Biomed Mater*. 2008;3(3):034101.

[50] Chen CY, Barron JA, Ringeisen BR. *Appl Surf Sci*. 2006;252(24):8641-8645.

[51] Serra P, Duocastella M, Fernández-Pradas JM, et al. *Appl Surf Sci*. 2009;255(10):5342-5345.

[52] Keriquel V, Oliveira H, Rémy M, et al. *Sci Rep*. 2017;7(1):1778.

[53] Serra P, Duocastella M, Fernández-Pradas JM, et al. *Cell Org Print*. 2010:53-80.

[54] Hopp B, Smausz T, Nógrádi A. *Cell Organ Prin*. 2010:115-134.

[55] Boutopoulos C, Kalpyris I, Serpetzoglou E, et al. *Microfluid Nanofluidics*. 2014;16:493-500.

[56] Doraiswamy A, Narayan RJ, Lippert T, et al. *Appl Surf Sci*. 2006;252(13):4743-4747.

[57] Catros S, Fricain JC, Guillotin B, et al. *Biofabrication*. 2011;3(2):025001.

[58] Koch L, Deiwick A, Franke A, et al. *Biofabrication*. 2018;10(3):035005.

[59] Smausz T, Hopp B, Kecskeméti G, et al. *Appl Surf Sci*. 2006;252(13):4738-4742.

[60] Koch L, Deiwick A, Chichkov B. *Bio Nanomater*. 2014;15(3-4):71-78.

[61] Lin Y, Huang Y, Chrisey DB. *J Biomech Eng*. 2011;133(2):025001.

[62] Xiong R, Zhang Z, Chai W, et al. *Biofabrication*. 2017;9(2):024103.

[63] Ventura RD. *Med Lasers Eng Basic Res Clin Appl*. 2021;10(2):76-81.

[64] Mandrycky C, Wang Z, Kim K, et al. *Biotechnol Adv*. 2016;34(4):422-434.

[65] de Mori A, Peña Fernández M, Blunn G, Et Al. *Polymers (Basel)*. 2018;10(3):285.

[66] Zhu J, Beamish JA, Tang C, et al. *Macromol*. 2006;39(4):1305-1307.

[67] O'Connell CD, Zhang B, Onofrillo C, et al. *Soft Matter*. 2018;14(11):2142-2151.

[68] Raman R, Bashir R. *Acad Press.* 2015:89-121.

[69] Li L, Fourkas JT. *Mater Today*. 2007;10(6):30-37.

[70] Sun C, Fang N, Wu DM, et al. *Sensor Actuat A Phys*. 2005;121(1):113-120.

[71] Raman R, Bhaduri B, Mir M, et al. *Adv Healthc Mater*. 2016;5(5):610-619.

[72] Andrews. *Harv Sci Rev. 1977.*

[73] Tang D, Tare RS, Yang LY, et al. *Biomaterials*. 2016;83:363-382.

[74] Miller JS, Stevens KR, Yang MT, et al. *Nat Mater*. 2012;11(9):768-774.

[75] Stoltz JF, Zhang L, Ye JS, et al. *Bio Medi Mater Eng*. 2017;28(s1):121-127.